Differential effects of lipids and lyso-lipids on the mechanosensitivity of the mechanosensitive channels MscL and MscS

Takeshi Nomura[a], Charles G. Cranfield[a,b], Evelyne Deplazes[c], Dylan M. Owen[d], Alex Macmillan[e], Andrew R. Battle[a,f], Maryrose Constantine[a], Masahiro Sokabe[g,h], and Boris Martinac[a,b,1]

[a]Molecular Cardiology and Biophysics Divison/Mechanosensory Biophysics Laboratory, Victor Chang Cardiac Research Institute, Darlinghurst, New South Wales 2010, Australia; [c]School of Biomedical, Biomolecular and Chemical Sciences, University of Western Australia, Nedlands, Western Australia 6009, Australia; [d]Centre for Vascular Research and [e]Biomedical Imaging Facility, University of New South Wales, Kensington, NSW 2052, Australia; [f]School of Pharmacy, Griffith University, Parklands, Queensland 4222, Australia; [g]International Cooperative Research Project/Solution Oriented Research for Science and Technology (ICORP/SORST) Cell Mechanosensing, Japan Science and Technology Agency (JST), Nagoya 466-8550, Japan; [h]Department of Physiology, Nagoya University Graduate School of Medicine, Nagoya 466-8550, Japan; and [b]St. Vincent's Clinical School, University of New South Wales, Sydney, New South Wales 2052, Australia

Edited* by Ching Kung, University of Wisconsin, Madison, WI, and approved April 18, 2012 (received for review January 4, 2012)

Mechanosensitive (MS) channels of small (MscS) and large (MscL) conductance are the major players in the protection of bacterial cells against hypoosmotic shock. Although a great deal is known about structure and function of these channels, much less is known about how membrane lipids may influence their mechanosensitivity and function. In this study, we use liposome coreconstitution to examine the effects of different types of lipids on MscS and MscL mechanosensitivity simultaneously using the patch-clamp technique and confocal microscopy. Fluorescence lifetime imaging (FLIM)-FRET microscopy demonstrated that coreconstitution of MscS and MscL led to clustering of these channels causing a significant increase in the MscS activation threshold. Furthermore, the MscL/MscS threshold ratio dramatically decreased in thinner compared with thicker bilayers and upon addition of cholesterol, known to affect the bilayer thickness, stiffness and pressure profile. In contrast, application of micromolar concentrations of lysophosphatidylcholine (LPC) led to an increase of the MscL/MscS threshold ratio. These data suggest that differences in hydrophobic mismatch and bilayer stiffness, change in transbilayer pressure profile, and close proximity of MscL and MscS affect the structural dynamics of both channels to a different extent. Our findings may have far-reaching implications for other types of ion channels and membrane proteins that, like MscL and MscS, may coexist in multiple molecular complexes and, consequently, have their activation characteristics significantly affected by changes in the lipid environment and their proximity to each other.

Escherichia coli | giant spheroplasts | liposomes | amphipaths | pressure clamp

Various types of mechanosensitive (MS) ion channels are present in membranes of eukaryotic and prokaryotic cells, where they function as molecular detectors of mechanical stimuli such as touch, sound, and gravity acting on membranes of living cells (1, 2). Among the best-studied MS channels to date are the bacterial channels of small (MscS) and large (MscL) conductance functioning as safety valves, which protect bacteria from rupturing upon a challenge by hypoosmotic shock (3).

It is well established that the biophysical properties of membrane proteins including ion channels are affected by their lipid environment (4, 5). Molecules such as cholesterol increase the bending modulus (6), as well as change the bilayer pressure profile (7) of the lipid bilayer and, hence, the channel gating properties. Other properties such as lipid tail length (8) and lipid head groups (9) affect the gating of MscL. Amphipathic molecules such as local anesthetics or the single-chain lipid lysophosphatidylcholine (LPC) also activate MscS and MscL by inducing curvature and change in the pressure profile in the lipid bilayer (8, 10, 11). A detailed mechanism of how lipids interact with these channels in the bacterial cell membrane and influence their mechanosensitivity remains poorly understood. For example, it remains unclear why the sensitivity of bacterial MS channels (MscL, MscS/MscK, MscM) to activation by membrane tension decreases with their conductance (12). Also, it is not clear why, unlike MscL, MscS has a tendency to concentrate at the poles in bacteria at frequencies correlated with the cellular cardiolipin content (13).

In this study, we have examined the effect of acyl chain length, cholesterol, and lyso-lipids on the mechanosensitivity of MscS and MscL coreconstituted into liposomes (14). This approach allowed us to freely change the ratio and type of lipids in liposome preparations and study the effect of these changes on the MscL/MscS threshold ratio (TR). TRs were determined by the pressure applied to patch pipettes (i.e., membrane tension) required for gating MscS and MscL by stretching the lipid bilayer. Our study investigates lipid–protein interactions by simultaneously examining two membrane ion channels coreconstituted into artificial liposomes of different lipid composition.

Results and Discussion

Comparison Between the Activation Threshold and the Activation Midpoint in Determining the Activation Ratio (MscL/MscS). Channel gating thresholds have been frequently used in the studies of bacterial MS channels to estimate the mechanosensitivity of MscS and MscL (15, 16). Instead of measuring the first channel opening of MscS and MscL to determine the TR, an alternative method is to calculate the midpoint ratio (MR) from an activation curve with the midpoints determined as the pressure (tension) at which instantaneous current is half of the current at saturation (17, 18). It remained unclear which pair of parameters characterizes better the difference in MscL and MscS tension sensitivities. To examine whether there is a difference between the TR and the MR for MscL and MscS, we compared them by using *Escherichia coli* giant spheroplasts and azolectin (100%) liposomal membranes, which contain both wild-type MscS and MscL. These observations indicate that there is little difference between the TR and the MR for MscS and MscL in the membrane bilayer composed of the same type of lipids (Fig. 1; for further details, see *SI Text*). When

Author contributions: T.N., C.G.C., A.R.B., and B.M. designed research; T.N., C.G.C., E.D., D.M.O., A.M., A.R.B., and M.C. performed research; B.M. contributed new reagents/analytic tools; T.N., C.G.C., E.D., D.M.O., and A.M. analyzed data; and T.N., C.G.C., A.R.B., M.S., and B.M. wrote the paper.

The authors declare no conflict of interest.

*This Direct Submission article had a prearranged editor.

[1]To whom correspondence should be addressed. E-mail: B.Martinac@victorchang.edu.au.

This article contains supporting information online at www.pnas.org/lookup/suppl/doi:10.1073/pnas.1200051109/-/DCSupplemental.

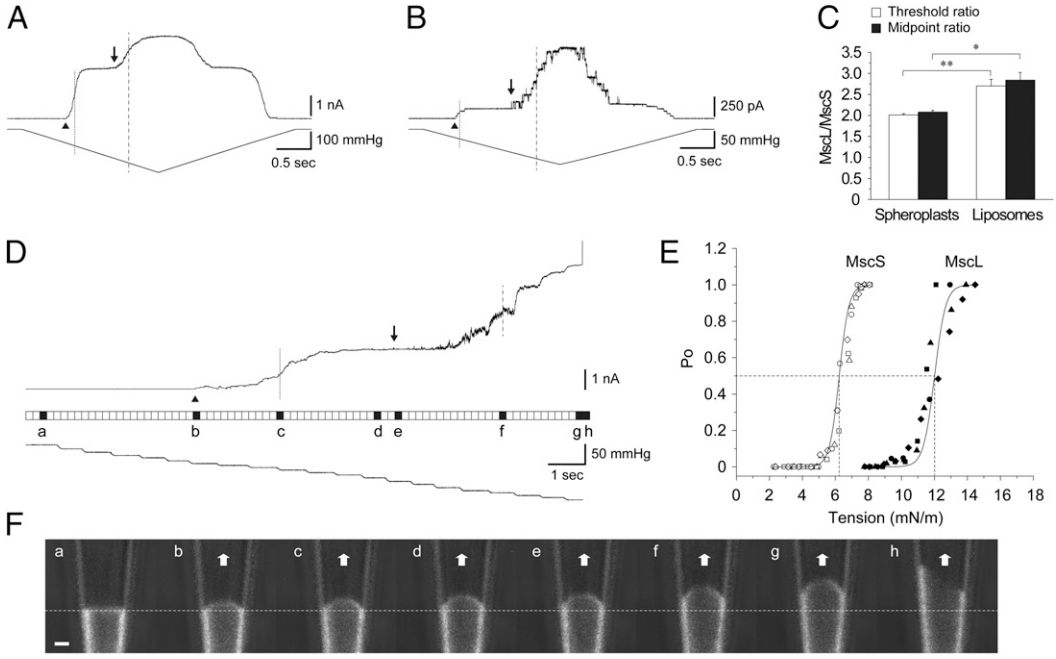

Fig. 1. Comparison of the TR and patch fluorescence confocal microscopy of MscS and MscL. Channel activities of MscS and MscL in spheroplasts (AW737) (*A*) and azolectin (100%) (*B*) liposomes. Arrowhead and arrow indicate the first opening of MscS and MscL, and dotted and dashed line show the midpoint activation of MscS and MscL, respectively. (*C*) TR and MR of MscS and MscL (mean ± SEM; $n = 6–7$). (*D*, *Top*) Representative current trace of MscS and MscL coreconstituted into azolectin (99.9%) and rhodamine-PE (0.1%) liposomes recorded at +30-mV pipette potential. The filled squares in *a*–*h* between the current and pressure trace indicate resting state (*a*), first channel opening of MscS (arrowhead) (*b*), midpoint activation of MscS (dotted line) (*c*), saturating point of MscS activity (*d*), first channel opening of MscL (arrow) (*e*), midpoint activation of MscL (dashed line) (*f*), saturating point of MscL activity (*g*), and lysis of the patch membrane (*h*), respectively. (*E*) Boltzmann curves for MscS and MscL. The midpoint tension for MscS and MscL is 6.2 ± 0.1 and 12.0 ± 0.3 mN/m, respectively (mean ± SEM; $n = 4$). These values correspond well to those values obtained previously by other researchers (48, 49). (*F*) Confocal single frame images of the patch membrane showing the shape of the patch membrane corresponding to the current traces shown in *D*. Scan rate was 196 ms/scan, with no interval between consecutive scans. Dashed line indicates the resting position of the patch membrane. (Scale bar: 1 μm.)

measuring the activation ratios for MscL compared with MscS, the TR method is preferable, because measuring the MR requires MscL activation to saturate before the membrane seal or patch is broken by the applied negative pressures. Consequently, most of the results in this study are based on determining the TR rather than the MR.

Effect of the Bilayer Thickness on MscS and MscL. MscL channel activity was reported to be strongly dependent on the thickness of the lipid bilayer in which the channel was reconstituted, such that decreasing bilayer thickness lowered MscL activation energy, whereas an increase in the bilayer thickness led to an increase in the MscL energy of activation (8). Similar results have not been reported for MscS.

To assess whether the difference in lipid acyl chain length affects mechanosensitivity and the MscL/MscS TR, we coreconstituted both channels into liposomes made of PE18:PC18 (70%:30%), PE16:PC16 (70%:30%), and azolectin. Current traces shown in Fig. 2 *A* and *B* represent the channel activity recorded from PE18:PC18 (70%:30%) and PE16:PC16 (70%:30%) liposomes, respectively. The activation threshold of MscL in PE16:PC16 (70%:30%) and PE18:PC18 (70%:30%) liposomes was lower compared with the threshold required for the channel activation in soybean azolectin (100%) liposomes (Fig. 2*C*). In contrast, the activation threshold of MscS in liposomes made of PE16:PC16 (70%:30%) and PE18:PC18 (70%:30%) was approximately the same as the threshold in azolectin (100%) liposomes (Table S1 and Fig. 2*C*). Consequently, the MscL/MscS TR decreased in the shorter PE16:PC16 compared with the longer PE18:PC18 lipids (Fig. 2*C*). Together, these results indicate that the molecular mechanism underlying the mechanosensitivity of MscS and MscL differs for the two channels in accordance with several previous reports (19–22).

The results suggest that, because of their very different molecular structure (23), lipid–protein interactions are different for the two channels. In the case of the MscL pentamer, the reduction of the thickness of the transmembrane portion of the channel following the reduction of the lipid bilayer thickness would be attained by a significant tilt of the TM1 and TM2 transmembrane helices (24) resulting in the opening of the very large channel pore of 30 Å in diameter (24, 25). In the case of the MscS heptamer a lesser tilt of the TM1 and TM2 helices is required to accommodate the smaller MscS open channel pore of 14–16 Å (19). Thus, it would seem an overall smaller conformational change is required for the closed-open transition in MscS compared with MscL resulting in MscS being apparently less sensitive to bilayer thinning.

Cholesterol Effects on Mechanosensitivity of MscS and MscL. Cholesterol has been shown to influence the function of numerous membrane proteins including ion channels (26). We coreconstituted MscL and MscS channels in azolectin liposomes containing different percentages of cholesterol (0–30%) to assess how the changes in the cholesterol may affect the mechanosensitivity of these channels.

It is a well-known fact that cholesterol influences the mechanical properties of the lipid bilayer of cell membranes by: (*i*) reducing bilayer fluidity, thus making it stiffer; (*ii*) decreasing its permeability, thereby affecting its thickness by increasing the orientational order of phospholipid molecules (27, 28); and (*iii*) affecting the transbilayer pressure profile (7). However, it has been shown that up to 40% cholesterol does not increase the bending modulus of membrane bilayers composed of phosphatidylcholine lipids with

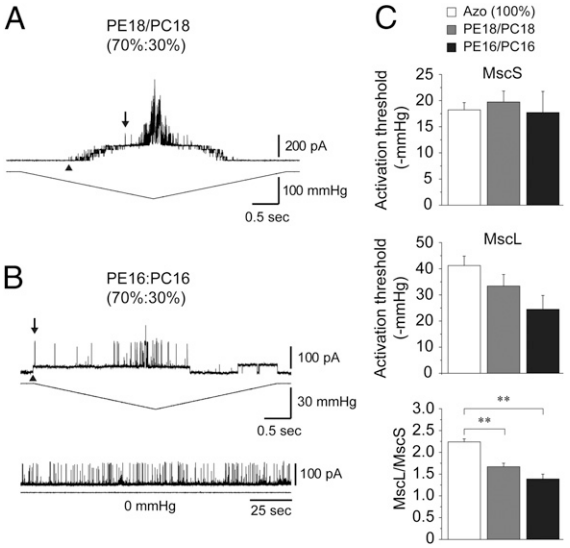

Fig. 2. Effects of bilayer thickness on coreconstituted MscS and MscL. (*A*) Current traces of MscS and MscL coreconstituted into PE18:PC18 (70%:30%) liposomes recorded at +30 mV. Arrowheads point to the first observed MscS opening, whereas the downward pointing arrows indicate the first observed MscL opening used to determine the MscL/MscS TR. (*B*) Representative current traces of MscS and MscL coreconstituted into PE16:PC16 (70%:30%) liposomes (*upper*) and spontaneous opening of MscL in the absence of pressure (*Lower*). Spontaneous openings were noticed in 2/16 patches and are most likely the result of induced membrane tension caused by the formation of the giga-ohm seal (50, 51). (*C*) Activation threshold of MscS *(Top)* and MscL *(Middle)* coreconstituted into azolectin (100%), PE18:PC18 (70%:30%), and PE16:PC16 (70%:30%) liposomes (mean ± SEM; $n = 7–8$). TR of MscL relative to MscS (mean ± SEM; $n = 7–8$) *(Bottom)*. Significant differences are indicated by asterisks (**$P < 0.01$ by *t* test).

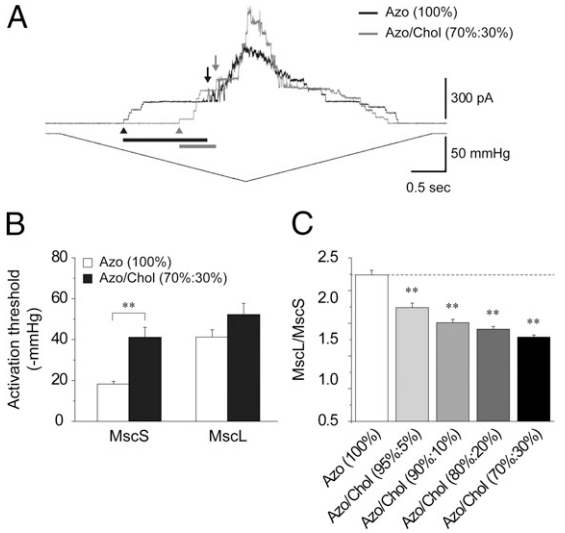

Fig. 3. Cholesterol effects on MscS and MscL. (*A*) Superimposed current traces (*Upper*) of MscS and MscL coreconstituted into azolectin (100%) and azolectin:cholesterol (70%:30%) liposomes in response to negative pressure (*Lower*) at +30 mV pipette voltage. Black and gray bars indicate the relative change in the activation threshold of MscS and MscL, respectively. First MscS (arrowhead) and MscL (arrow) opening are indicated. (*B*) Activation threshold of MscS and MscL coreconstituted into azolectin (100%) and azolectin:cholesterol (70%:30%) liposomes (mean ± SEM; $n = 9–15$). Significant differences are indicated by asterisks in *B* and *C* (**$P < 0.01$ by *t* test). (*C*) TR of MscL and MscS reconstituted in azolectin 100% and azolectin: cholesterol 95%:5%, 90%:10%, 80%:20%, and 70%:30% liposomes (mean ± SEM; $n = 9–15$).

two monounsaturated chains, although it does have the expected stiffening effect on membranes composed of lipids with two saturated chains (29). Therefore, the effect of cholesterol on lipid bilayers is not universal since it depends on the saturation of aliphatic carbon tails. In this context we note that azolectin liposomes in our experiments consisted of phospholipids containing the carbon chains C16:0, C18:0, C18:2, and C18:3 of which the C18:2 comprised 60% (30). It has been suggested that because cholesterol has a smooth face and a rough face due to two bulky methyls sticking out on the same rough side of the otherwise puckered ring structure, saturated chains should be more likely to pack against the smooth face which then acts to condense them into straighter chains taking up considerably less area. Cholesterol interaction with unsaturated aliphatic carbon chains would therefore be much weaker, making the unsaturated chains less susceptible to condensing (29). Consequently, the effects of cholesterol on MscL and MscS we observed in azolectin liposomes result most likely from the interaction of cholesterol with the saturated phospholipids in azolectin through a change in bilayer thickness, stiffness and/or transbilayer pressure profile.

Fig. 3*A* shows superimposed current traces of MscS and MscL coreconstituted into liposomes made of azolectin (100%) (*black trace*) and azolectin/cholesterol (70%:30%) (*gray trace*). Higher membrane tension was required to activate both channels in the presence of cholesterol. The relative increase in activation threshold of MscS was much higher (126%) compared with MscL (27%) (Fig. 3*B*) indicating a much stronger effect of cholesterol on MscS. Overall, the addition of 5–30% cholesterol led to a decrease of the MscL/MscS TR (Fig. 3*C*).

Since the total membrane-associated area (i.e., the buried protein area in contact with the interior of the lipid bilayer) of MscL is 140 nm^2 (1) stiffening of the bilayer can be expected to reduce the freedom of movement of MscL transmembrane helices and thus reducing the mechanosensitivity of the channel. However, given that MscL mechanosensitivity was shown to be significantly dependent on the bilayer thickness (8) change in hydrophobic mismatch is more likely to contribute to the increase in the MscL activation threshold (Fig. 3*B*).

MscS exhibited a much larger increase in the pressure activation threshold in azolectin/cholesterol liposomes compared with that of MscL (Fig. 3*B*). The decrease in its fluidity (29) may be the major factor causing this increase: (*i*) the total membrane-associated area of MscS of 300 nm^2 (31) is much larger compared with that of MscL; and (*ii*) MscS exhibits a significant reduction in activity attributable to lateral compression of the bilayer under high hydrostatic pressure (31). Given that hydrophobic mismatch seems to have less influence on MscS activity (Fig. 2*C*), bilayer stiffness could be the main factor affecting it, while hydrophobic mismatch appears to be more important for MscL.

In addition to the factors discussed above, we cannot exclude the possibility that cholesterol could influence both MscL and MscS through specific interactions with them given that other ion channels such as inwardly rectifying K^+ channels were shown to be sensitive to specific sterol- channel protein interactions (26). However, it is more likely it is its effect on the transbilayer pressure profile (7) that is affecting both channels. The pressure profile across the bilayer is a result of the contracting influence of the head groups balanced by the tendency of the lipid tails to maximize their entropy by occupying a greater volume (7, 32). A scanning mutagenesis study suggested that the amino acids of the mechanosensing regions of MscS were located at both periplasmic and cytoplasmic ends of TM1 and TM2 transmembrane helices (20). Similarly, a genetic study isolating suppressors of gain-of-function mutants (33) together with scanning-mutagenesis studies (21, 34) identified amino acids forming the "mechanosensor" of MscL at the periplasmic border of the lipid–protein interface, although other studies indicated that mechanosensing in

MscL is also occurring at the cytoplasmic interface (35) portions of the pore and mid-TM2 (36). Theoretical considerations provide lateral pressures in the bilayer core of about 350 atm, whereas the contracting surface tension resulting from hydrophilic head groups being squeezed together to prevent exposure of the hydrophobic tails to the aqueous compartment in each monolayer is on the order of 1000 atm (32). The contracting influence of the lipid head groups near the aqueous interface affecting the mechanosensing regions of MscS and MscL is expected to induce a change in the transbilayer pressure profile and so have an effect on the closed – open equilibrium of both MscL and MscS. This interpretation is in line with the findings of several studies suggesting that lipid effects on MS channel activity act through changes in the biophysical properties of the lipid bilayer, rather than through specific lipid–protein interactions (9, 32).

Activation of MscS and MscL by LPC. It has been reported that amphipathic compounds including the single-tailed lyso-lipid LPC activate bacterial MS channels by intercalating into one of the bilayer leaflets (8, 10, 11). A coarse-grained simulation study (37) suggested that asymmetric incorporation of LPC into the membrane bilayer should curve the bilayer such that the higher the local LPC concentration, the higher the local curvature frustration. This is in agreement with structural electron paramagnetic resonance experiments showing that only asymmetrically incorporated LPC into a membrane bilayer could activate MscL, whereas symmetrically inserted LPC did not have any effect (8). A detailed analysis of the geometrical and mechanical properties of the curved bilayers indicated that the packing of phosphate groups (i.e., area-per-lipid) rather than local curvature is the cause of the large variation in the local pressure profile affecting the MS channels (37).

To tease out similarities and differences between the effect of amphipaths on MscL and MscS coreconstituted in the same lipid bilayer, we used LPC to open the channels in azolectin (100%) liposomes. Because it has been reported previously that the liposome membrane could creep up along the wall of the patch pipette as a result of the ionic strength of the recording solution, leading to an increase in the resting tension of the liposome patch (38), before the LPC experiments, we determined the extent of creeping of liposome patches with time in our experiments (see *SI Text*). Fig. 4*A* shows current traces of MscS and MscL recorded in the absence of LPC upon application of pressure ramps before and after a 10 min interval, which was sufficient to determine reliably the LPC effect before and after its application. The activation threshold before application of LPC decreased over that interval 15% for MscS and 10% for MscL.

Application of LPC to the liposome patch caused spontaneous channel activity after approximately 10 min (Fig. 4*B*). MscS was activated first, followed by brief openings of MscL. Again, we applied a pressure ramp and noticed a 75% reduction in the activation threshold of MscS and 57% in the activation threshold of MscL (Fig. 4*C*), resulting in a significant increase in the MscL/MscS TR (Fig. 4*D*). As was the case with cholesterol, LPC also exerted a larger effect on MscS than on MscL.

MscS and MscL can be activated not only by suction but also when positive pressure is applied to a giant spheroplast at the pipette tip in whole-spheroplast mode (39, 40). Given that the channel activity increased with the decrease in the curvature in whole-spheroplast mode, curvature is unlikely to be a stimulus gating the channels. Nevertheless, incorporation of amphipathic molecules could facilitate opening of the MS channels (9, 10) possibly by affecting the packing of phosphate groups, which could cause change in the local pressure profile in the lipid bilayer (37).

Clustering of MscL and MscS. To determine whether coreconstitution has an effect on the activation TR, we measured the membrane tension thresholds for MscS and MscL separately and coreconstituted using patch fluorescence confocal microscopy (see *SI Text*). Results show a significant increase in the membrane tension threshold for MscS when coreconstituted with MscL. There was an increase in the MscL activation threshold in the coreconstituted patches, but it was not significantly different (Fig. 5*A*). As previously reported (17), MscL clusters with other MscL molecules and computational modeling has suggested that this clustering has a significant impact on the free energy needed to open the channel (41). We conducted a fluorescence lifetime imaging (FLIM)-FRET experiment to determine whether MscS and MscL preferentially cluster together within lipids. To do this, we separately labeled an MscL M94C mutant with a donor fluorophore Alexa Fluor 488 (AF488) and an MscS M47C mutant with an acceptor fluorophore Alexa Fluor 568 (AF568). Both point cysteine mutations are localized on the outer transmembrane region of their respective proteins (Fig. 5*B*). In regions of clustering

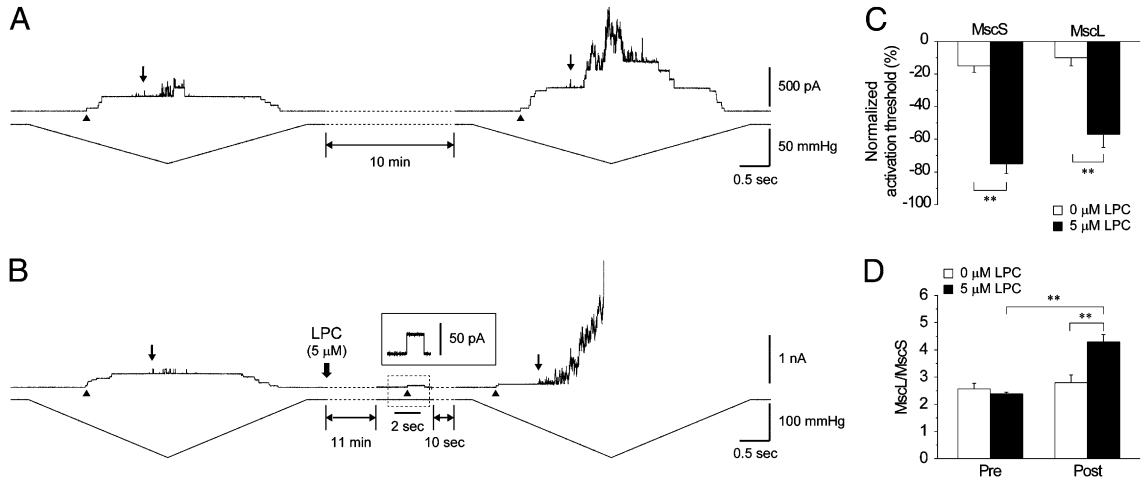

Fig. 4. LPC effect on MscS and MscL. (*A*) MscS and MscL activation thresholds were recorded by applying pressure ramps for 10 min after *training* the patch. After another 10 min, the pressure ramp was reapplied. First MscS (arrowhead) and MscL (arrow) opening are indicated. (*B*) LPC (5 μM) was applied to the bath after the 10-min interval. *Inset* shows a single channel trace of MscS at +30-mV pipette voltage. (*C*) Normalized activation threshold of MscS and MscL coreconstituted into azolectin (100%) liposomes before and after 10-min interval in the absence and presence of 5 μM LPC (mean ± SEM; $n = 5$). (*D*) TR before and after addition of 0 and 5 μM LPC (mean ± SEM; $n = 5$). Significant differences are indicated by asterisks in *C* and *D* (**$P < 0.01$ by *t* test).

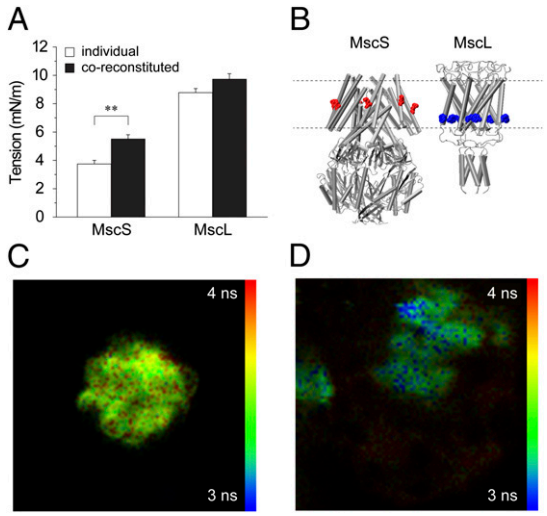

Fig. 5. Clustering of MscS with MscL. (*A*) MscS and MscL activation thresholds were measured for individually reconstituted or coreconstituted channels (mean ± SEM; $n = 6–9$). The difference was significant for MscS (**$P < 0.01$ by t test). (*B*) Illustration of the two labeled proteins with the approximate position of each fluorescent label. MscS was labeled with AF568 (acceptor), whereas MscL was labeled with AF488 (donor). (*C*) FLIM image (70 × 70 μm) of an azolectin (100%) sample reconstituted with a donor only population of MscL M94C labeled with AF488. (*D*) FLIM image of azolectin (100%) sample containing separate populations of MscL M94C labeled with AF488 and MscS M47C labeled with AF568. Lifetimes are measured for the donor fluorophore (AF488) only. Regions colored in blue show areas where fluorescence lifetimes are shorter as a result of FRET attributable to the close proximity of the MscL and MscS protein populations in the lipid, indicating clustering. FRET is not exhibited uniformly in all regions of the lipid.

between the two protein populations, the fluorescence lifetime of the donor population will be reduced because of the close proximity of the acceptor population due to resonance transfer. For completeness, it was also necessary to determine whether MscS would cluster with itself. We separately labeled two populations of MscS M47C, one with just the donor and one with just the acceptor and then followed a similar reconstitution protocol.

Compared with an MscL donor only sample (Fig. 5*C*), in the mixed MscS and MscL samples, we were able to distinguish selected regions of reduced fluorescence lifetimes in our samples indicative of self-assembly into clusters for our labeled proteins (Fig. 5*D*). This result suggests that it is energetically favorable for MscS to cluster with MscL proteins in lipid membranes. In contrast, no clustering could be detected for MscS with itself in any of our samples. It was suggested that MscS may induce midplane bending in the surrounding lipids (4); then, the fact that no evidence could be found to show that MscS clusters with itself is consistent with an earlier proposition that all MscS molecules are oriented in the same direction in the lipid bilayer, (*SI Text*). Midplane bending of the lipids surrounding like-oriented proteins would mean it is energetically favorable for the proteins to repel each other (4). Oppositely oriented proteins on the other hand should attract. MscL has previously been shown to be oriented in the same direction in liposome membrane patches (42). Given the uniform orientation of MscL in liposome bilayers, it is feasible to assume that MscS uniform orientation could also be facilitated by the uniform MscL orientation. In the case of MscL clustering, it is thickness deformation that may be the driving force for induced self-assembly into clusters (4, 41). Based on these data, it seems reasonable that it is the close association between MscS and MscL in the patch membrane that is causing the increase in activation thresholds for MscS in the coreconstituted liposome patches.

Conclusions

Interactions with their lipid environment is particularly important for MS channel function, because they are gated by the bilayer tension (43). The coreconstitution of MscL and MscS enabled us to demonstrate that the differences in the lipid environment affected the channels individually and to an extent related to their particular molecular structure. Most importantly, the activation properties of the channels are significantly affected by their clustering. Our study suggests that by changing the lipid composition of their cell membranes (44), bacteria may be able to broaden the repertoire of mechanisms they can use to modulate the activity of MS channels and, thus, more successfully adjust to potentially life-threatening changes in the osmolarity of their habitats. The study also has important implications for other membrane proteins including biological channels and transporters that may coexist in multiple molecular complexes.

Materials and Methods

Chemicals. Chloroform, cholesterol, soybean azolectin, KCl, $MgCl_2$, Hepes, *n*-dodecyl β-D-maltoside (DDM) and KOH were all obtained from Sigma-Aldrich. BioBeads were purchased from Bio-Rad, whereas 1,2-dioleoyl-*sn*-glycero-3-phosphoethanolamine (DOPE) (PE18:1), 1,2-dipalmitoleoyl-*sn*-glycero-3-phosphoethanolamine (PE16:1), 1,2-dioleoyl-*sn*-glycero-3- phosphocholine (DOPC) (PC18:1), 1,2-dipalmitoleoyl-*sn*-glycero-3-phosphocholine (PC16:1), and 1-oleoyl-2-hydroxy-*sn*-glycero-3-phosphocholine (18:1) were obtained as powders from Avanti Polar Lipids. All lipids were dissolved and stored in $CHCl_3$ at −30 °C. Doubly distilled water was used in all experiments.

Purification and Protein Incorporation into Liposomes. GST-MscL-WT and His_6-MscS-WT were prepared according to published procedures [MscL (45) and MscS (46)]. MscS and MscL were both incorporated into liposomes made of a single type of lipids or a lipid mixture (*Results*) using either a sucrose (14) or dehydration/rehydration (D/R) reconstitution method (45). See *SI Text* for more detail.

Electrophysiology. The channel activities of MscS and MscL were examined in liposomes, as well as in *E. coli* giant spheroplasts, using the patch-clamp method. Giant spheroplasts were prepared as described previously (47). Currents were amplified with an AxoPatch 1D amplifier (Axon Instruments), and data were acquired at a sampling rate of 5 kHz with 2-kHz filtration. The bath and pipette recording solution used in liposome experiments was the same consisting of 200 mM KCl, 40 mM $MgCl_2$, and 5 mM Hepes, whereas in spheroplast experiments the bath solution consisted of 250 mM KCl, 90 mM $MgCl_2$, and 5 mM Hepes (pH 7.2 adjusted with KOH). See *SI Text* for more details on patch-clamp electrophysiology methods and patch fluorescence confocal microscopy methods.

FLIM-FRET. FLIM was performed on a PicoQuant MicroTime 200 inverted confocal microscope with a 60×, 1.2-NA water-immersion objective. Excitation was via a fiber-coupled, pulsed laser diode operating at 470 nm with a pulse width below 200 ps. Detection was in the range 489–531 nm using a single-photon avalanche diode (SPAD) (MicroPhoton Devices) connected to time-correlated single-photon counting (TCSPC) electronics (PicoHarp 300; PicoQuant). Fluorescence decays from each pixel were fitted to a single exponential decay model to determine the fluorescence lifetimes, which were then displayed as a pseudocolored FLIM image. Additional FLIM-FRET experiments are shown in *SI Text*.

ACKNOWLEDGMENTS. We thank Paul Rohde and Mark Hunter for technical assistance. We also thank Dr. Reinhard Krämer for critical reading of the manuscript. This study was supported by Australian Research Council Grant DP0769983, National Health and Medical Research Council of Australia Grant 635525, and the Yamada Science Foundation.

1. Hamill OP, Martinac B (2001) Molecular basis of mechanotransduction in living cells. *Physiol Rev* 81:685–740.

2. Coste B, et al. (2012) Piezo proteins are pore-forming subunits of mechanically activated channels. *Nature* 483:176–181.

3. Levina N, et al. (1999) Protection of Escherichia coli cells against extreme turgor by activation of MscS and MscL mechanosensitive channels: Identification of genes required for MscS activity. *EMBO J* 18:1730–1737.
4. Phillips R, Ursell T, Wiggins P, Sens P (2009) Emerging roles for lipids in shaping membrane-protein function. *Nature* 459:379–385.
5. Fuster D, Moe OW, Hilgemann DW (2004) Lipid- and mechanosensitivities of sodium/hydrogen exchangers analyzed by electrical methods. *Proc Natl Acad Sci USA* 101: 10482–10487.
6. Needham D, Nunn RS (1990) Elastic deformation and failure of lipid bilayer membranes containing cholesterol. *Biophys J* 58:997–1009.
7. Cantor RS (1999) Lipid composition and the lateral pressure profile in bilayers. *Biophys J* 76:2625–2639.
8. Perozo E, Kloda A, Cortes DM, Martinac B (2002) Physical principles underlying the transduction of bilayer deformation forces during mechanosensitive channel gating. *Nat Struct Biol* 9:696–703.
9. Moe P, Blount P (2005) Assessment of potential stimuli for mechano-dependent gating of MscL: Effects of pressure, tension, and lipid headgroups. *Biochemistry* 44: 12239–12244.
10. Martinac B, Adler J, Kung C (1990) Mechanosensitive ion channels of E. coli activated by amphipaths. *Nature* 348:261–263.
11. Vásquez V, Sotomayor M, Cordero-Morales J, Schulten K, Perozo E (2008) A structural mechanism for MscS gating in lipid bilayers. *Science* 321:1210–1214.
12. Kung C, Martinac B, Sukharev S (2010) Mechanosensitive channels in microbes. *Annu Rev Microbiol* 64:313–329.
13. Romantsov T, Battle AR, Hendel JL, Martinac B, Wood JM (2010) Protein localization in Escherichia coli cells: Comparison of the cytoplasmic membrane proteins ProP, LacY, ProW, AqpZ, MscS, and MscL. *J Bacteriol* 192:912–924.
14. Battle AR, Petrov E, Pal P, Martinac B (2009) Rapid and improved reconstitution of bacterial mechanosensitive ion channel proteins MscS and MscL into liposomes using a modified sucrose method. *FEBS Lett* 583:407–412.
15. Blount P, Sukharev SI, Schroeder MJ, Nagle SK, Kung C (1996) Single residue substitutions that change the gating properties of a mechanosensitive channel in Escherichia coli. *Proc Natl Acad Sci USA* 93:11652–11657.
16. Blount P, Moe PC (1999) Bacterial mechanosensitive channels: Integrating physiology, structure and function. *Trends Microbiol* 7:420–424.
17. Chiang CS, Anishkin A, Sukharev S (2004) Gating of the large mechanosensitive channel in situ: Estimation of the spatial scale of the transition from channel population responses. *Biophys J* 86:2846–2861.
18. Belyy V, Anishkin A, Kamaraju K, Liu N, Sukharev S (2010) The tension-transmitting 'clutch' in the mechanosensitive channel MscS. *Nat Struct Mol Biol* 17:451–458.
19. Booth IR, Edwards MD, Black S, Schumann U, Miller S (2007) Mechanosensitive channels in bacteria: Signs of closure? *Nat Rev Microbiol* 5:431–440.
20. Nomura T, Sokabe M, Yoshimura K (2006) Lipid-protein interaction of the MscS mechanosensitive channel examined by scanning mutagenesis. *Biophys J* 91:2874–2881.
21. Yoshimura K, Nomura T, Sokabe M (2004) Loss-of-function mutations at the rim of the funnel of mechanosensitive channel MscL. *Biophys J* 86:2113–2120.
22. Booth IR, et al. (2011) Sensing bilayer tension: Bacterial mechanosensitive channels and their gating mechanisms. *Biochem Soc Trans* 39:733–740.
23. Steinbacher S, Bass R, Strop P, Rees DC (2007) Structures of the prokaryotic mechanosensitive channels MscL and MscS. *Mechanosensitive Ion Channels, Part A*, Current Topics in Membranes (Elsevier Academic Press Inc, San Diego), Vol 58, pp 1–24.
24. Perozo E, Cortes DM, Sompornpisut P, Kloda A, Martinac B (2002) Open channel structure of MscL and the gating mechanism of mechanosensitive channels. *Nature* 418:942–948.
25. Cruickshank CC, Minchin RF, Le Dain AC, Martinac B (1997) Estimation of the pore size of the large-conductance mechanosensitive ion channel of Escherichia coli. *Biophys J* 73:1925–1931.
26. Levitan I, Fang Y, Rosenhouse-Dantsker A, Romanenko V (2010) Cholesterol and ion channels. *Cholesterol Binding and Cholesterol Transport Proteins, Subcellular Biochemistry*, ed Harris JR (Springer, Dordrecht, The Netherlands), Vol 51, pp 509–549.
27. Cooper RA (1978) Influence of increased membrane cholesterol on membrane fluidity and cell function in human red blood cells. *J Supramol Struct* 8:413–430.
28. Ipsen JH, Mouritsen OG, Bloom M (1990) Relationships between lipid membrane area, hydrophobic thickness, and acyl-chain orientational order. The effects of cholesterol. *Biophys J* 57:405–412.
29. Pan J, Tristram-Nagle S, Nagle JF (2009) Effect of cholesterol on structural and mechanical properties of membranes depends on lipid chain saturation. *Phys Rev E Stat Nonlin Soft Matter Phys* 80:021931.
30. Martinac B, Hamill OP (2002) Gramicidin A channels switch between stretch activation and stretch inactivation depending on bilayer thickness. *Proc Natl Acad Sci USA* 99: 4308–4312.
31. Macdonald AG, Martinac B (2005) Effect of high hydrostatic pressure on the bacterial mechanosensitive channel MscS. *Eur Biophys J* 34:434–441.
32. Gullingsrud J, Schulten K (2004) Lipid bilayer pressure profiles and mechanosensitive channel gating. *Biophys J* 86:3496–3509.
33. Li Y, Wray R, Blount P (2004) Intragenic suppression of gain-of-function mutations in the Escherichia coli mechanosensitive channel, MscL. *Mol Microbiol* 53:485–495.
34. Levin G, Blount P (2004) Cysteine scanning of MscL transmembrane domains reveals residues critical for mechanosensitive channel gating. *Biophys J* 86:2862–2870.
35. Iscla I, Wray R, Blount P (2011) An in vivo screen reveals protein-lipid interactions crucial for gating a mechanosensitive channel. *FASEB J* 25:694–702.
36. Maurer JA, Dougherty DA (2001) A high-throughput screen for MscL channel activity and mutational phenotyping. *Biochimica et Biophysica Acta (BBA) -. Biomembranes* 1514:165–169.
37. Yoo J, Cui Q (2009) Curvature generation and pressure profile modulation in membrane by lysolipids: Insights from coarse-grained simulations. *Biophys J* 97:2267–2276.
38. Suchyna TM, Sachs F (2007) Mechanosensitive channel properties and membrane mechanics in mouse dystrophic myotubes. *J Physiol* 581:369–387.
39. Cui C, Smith DO, Adler J (1995) Characterization of mechanosensitive channels in Escherichia coli cytoplasmic membrane by whole-cell patch clamp recording. *J Membr Biol* 144:31–42.
40. Belyy V, Kamaraju K, Akitake B, Anishkin A, Sukharev S (2010) Adaptive behavior of bacterial mechanosensitive channels is coupled to membrane mechanics. *J Gen Physiol* 135:641–652.
41. Grage SL, et al. (2011) Bilayer-mediated clustering and functional interaction of MscL channels. *Biophys J* 100:1252–1260.
42. Ajouz B, Berrier C, Besnard M, Martinac B, Ghazi A (2000) Contributions of the different extramembranous domains of the mechanosensitive ion channel MscL to its response to membrane tension. *J Biol Chem* 275:1015.
43. Kung C (2005) A possible unifying principle for mechanosensation. *Nature* 436: 647–654.
44. Yano Y, Nakayama A, Ishihara K, Saito H (1998) Adaptive changes in membrane lipids of barophilic bacteria in response to changes in growth pressure. *Appl Environ Microbiol* 64:479–485.
45. Häse CC, Le Dain AC, Martinac B (1995) Purification and functional reconstitution of the recombinant large mechanosensitive ion channel (MscL) of Escherichia coli. *J Biol Chem* 270:18329–18334.
46. Vásquez V, Cortes DM, Furukawa H, Perozo E (2007) An optimized purification and reconstitution method for the MscS channel: Strategies for spectroscopical analysis. *Biochemistry* 46:6766–6773.
47. Martinac B, Buechner M, Delcour AH, Adler J, Kung C (1987) Pressure-sensitive ion channel in Escherichia coli. *Proc Natl Acad Sci USA* 84:2297–2301.
48. Sukharev S (2002) Purification of the small mechanosensitive channel of Escherichia coli (MscS): The subunit structure, conduction, and gating characteristics in liposomes. *Biophys J* 83:290–298.
49. Sukharev SI, Sigurdson WJ, Kung C, Sachs F (1999) Energetic and spatial parameters for gating of the bacterial large conductance mechanosensitive channel, MscL. *J Gen Physiol* 113:525–540.
50. Suchyna TM, Markin VS, Sachs F (2009) Biophysics and structure of the patch and the gigaseal. *Biophys J* 97:738–747.
51. Ursell T, Agrawal A, Phillips R (2011) Lipid bilayer mechanics in a pipette with glass-bilayer adhesion. *Biophys J* 101:1913–1920.